Supporting information (SI)

A Self-assembled Graphene and $LiFePO_4$ Composite with Superior High Rate Capability for Lithium Ion Batteries

Wen-Bin Luo[a, b, c], **Shu-lei Chou**[b*], **Yu-Chun Zhai**[a*], **Hua-kun Liu**[b,c]

[a]School of Materials and Metallurgy, Northeastern University, Shenyang 110004, China. E-mail: zhaiyc@smm.neu.edu.cn.

[b]Institute for Superconducting and Electronic Materials, University of Wollongong, Wollongong, NSW 2522 Australia. E-mail: shulei@uow.edu.au.

[c]ARC Centre of excellence for Electromaterials Science, University of Wollongong, Wollongong, NSW 2522 Australia

Experimental

Synthesis

Graphene oxide (GO) was synthesized from graphite (Aldrich, powder, <20nm, synthetic) by Hummers method, the details of which have been described elsewhere. [1] Pure $LiFePO_4$ was prepared via the hydrothermal route from raw materials $FeSO_4{\cdot}7H_2O$, H_3PO_4, and $LiOH{\cdot}H_2O$ in a molar ratio of 1:1:3. First, LiOH aqueous solution was mixed with H_3PO_4 dopewise at vigorous agitation to form white suspension completely in 60 °C water bath for 40 min, and then agitate for 30 min at room temperature. A mixing solution of $FeSO_4{\cdot}7H_2O$ and citric acid (0.1 % weight of $FeSO_4{\cdot}7H_2O$) was added to the suspension. After stirring for 1 min, this suspension (~240 mL) was transferred into a stainless steel autoclave (inside volume 300 ml), and then reacted at 180 °C for 10 min in argon atmosphere. After reaction, the resultant light-green precipitation was collected, washed by water and ethanol for several times, and dried at 80 °C in vacuum. The obtained $LiFePO_4$ nanoparticles (0.4 g) were further dispersed into ethanol (200 ml) via sonication. After 1 h, 2 ml of aminopropyltrimethoxysilane (APS) was poured into the above solution and refluxed for 12 h under argon gas to obtain APS-modified nanoparticles. Finally the resultant precipitation was collected, washed by water several times. Graphene oxide encapsulated $LiFePO_4$ (LFP@GO) was fabricated via self-assemble to form peptide bonds between APS-modified $LiFePO_4$ and graphene oxide in aqueous solution. In a typical process, 200 ml APS-modified $LiFePO_4$ dispersion (2.0 $mg{\cdot}ml^{-1}$) was added into a 40 ml aqueous graphene oxide suspension (～0.5 $mg{\cdot}ml^{-1}$) under mild magnetic stirring 2 hours with pH 6.0. The LFP@GO was obtained after centrifugation and washing with water. Then, the obtained brown powder was dried at 60 °C for 10 h in a vacuum oven, followed by sintering at 600 °C for 3 h under Ar/H_2 (95:5,v/v) atmosphere to yield the graphene encapsulated $LiFePO_4$ (LFP@G). As a reference, the hydrothermally as-prepared $LiFePO_4$ was mixed with glucose, dried and treated at 600 °C for 3 h under Ar/H_2 atmosphere to yield carbon coated $LiFePO_4$ (LFP@C). Scheme 1 shows the synthesis process of materials. Micro- or nano-particles are firmly encapsulated with graphene oxide with peptide bonds.

Characterization

The phase purity and the structural characterization were analyzed by X-ray powder diffraction (GBC MMA) equipped with Cu Kα radiation that was operated over a 2θ range of 5～80° in a continuous scan mode with a scan rate of 2° min^{-1}. The particle size and morphology of the samples were examined using field emission scanning electron microscope (FE-SEM; JEOL JSM-7500). Transmission electron microscopy (TEM) investigations were performed using a 200 kV JEOL 2011. Raman spectra were performed using a Raman spectrometer (Jobin Yvon HR800) employing a 10 mW/neon laser at 632.8 nm. FTIR spectra were performed using a FTIR Prestige-21 (Shimadzu). X-ray photoelectron spectroscopy (XPS) experiments were carried out on a VG Scientific ESCALAB 2201XL instrument using aluminium Ka X-ray radiation during XPS analysis. XPS spectra analysis was done using XPS Peak-fit software. The amount of carbon and graphene in the samples was estimated using a Mettler-Toledo thermogravimetric analysis/differential scanning calorimetry (TGA/DSC) Stare System from 50-800 °C at 10 °C min^{-1} in air flux.

Electrochemical measurement

Electrochemical experiments were performed using CR2032 type coin cells. For preparing working electrodes, a mixture of the as-synthesized hybrid materials, carbon black, and poly(vinyl difluoride) (PVDF) at a weight ratio of 80:10:10, using 1-methyl-2-pyrrolidinone (NMP) as the solvent, was pasted on pure Al foil. Typical loadings of cathode powder with 150μm thickness were ～2 mg cm^{-2}. Microporous polypropylene separator (Celegard 2400) was used as a separator. The electrolyte consisted of a solution of 1 M $LiPF_6$ in ethylene carbonate (EC)/dimethyl carbonate (DMC) (1:1, in volume) obtained from Novolyte Chemical Co. Ltd. Pure lithium foil was used as a counter electrode. The cells were assembled in an argon-filled glove-box (Mbraun, Germany). Galvanostatic charge-discharge cycles were tested by LAND CT 2001A multi-channel battery testers at various current densities from 1 to 50 C (1C = 170 mAh.g^{-1}) between 4.2 and 2.0 V *vs.* Li^+/Li at room temperature. Measurements were repeated at least three times to ensure reliability, and EIS tests (Princeton Applied Research PARSTAT 2273) were conducted at a 3.41 V state of discharge with an AC amplitude of 10 mV in the frequency range 100 kHz to 10 mHz. The EIS data were collected from coin cells with lithium foil serving as both the counter and reference electrodes. EIS tests at different temperature including 20, 40, 50, and 60 °C were used to evaluate cell impedance and apparent activation energies. Cyclic voltammeter (CV) was conducted by using Princeton Applied Research PARSTAT 2273 at different scanning rate of 0.1, 0.2 , 0.5 , 1 , and 2 $mV\cdot s^{-1}$ between 2.0 and 4.2 V to evaluate Lithium ion diffusion coefficient ($D_{Li}{}^{+}$).

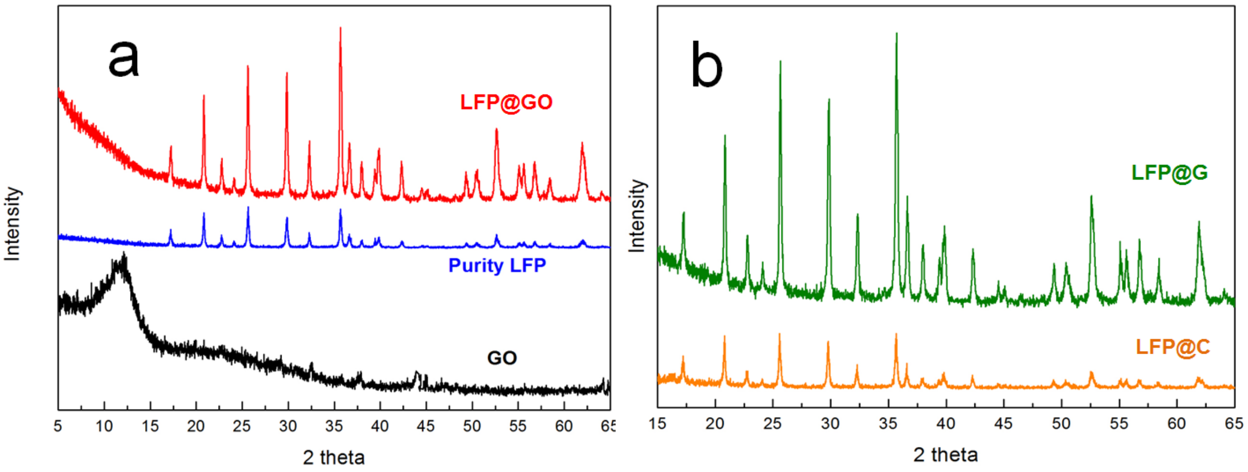

Figure S1. XRD patterns of the (a) GO, Pure LFP and LFP@GO composite; (b) LFP@C and LFP@G;

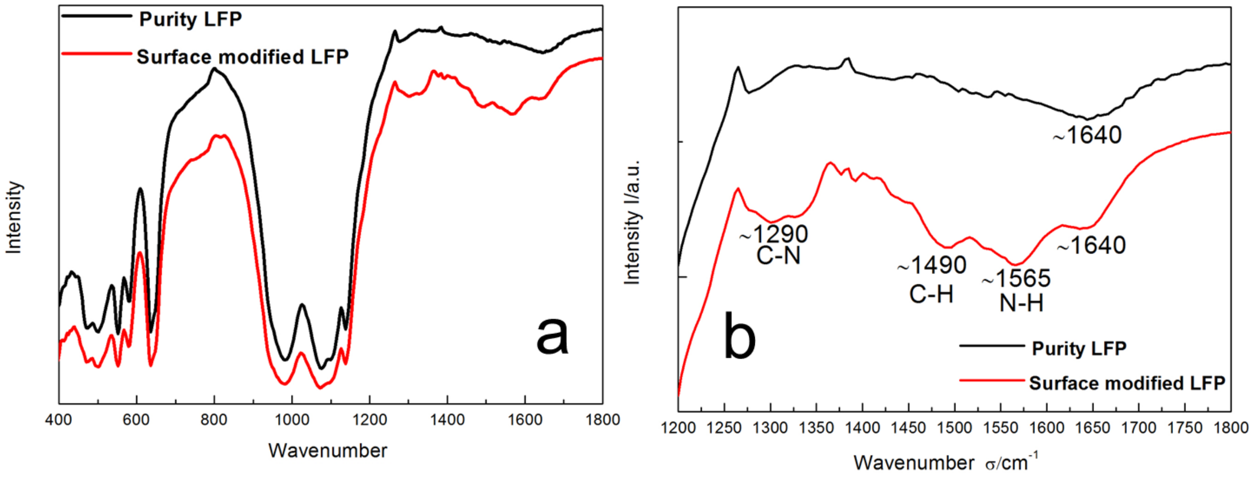

Figure S2. FT-IR results of Pure LFP and surface modified LFP

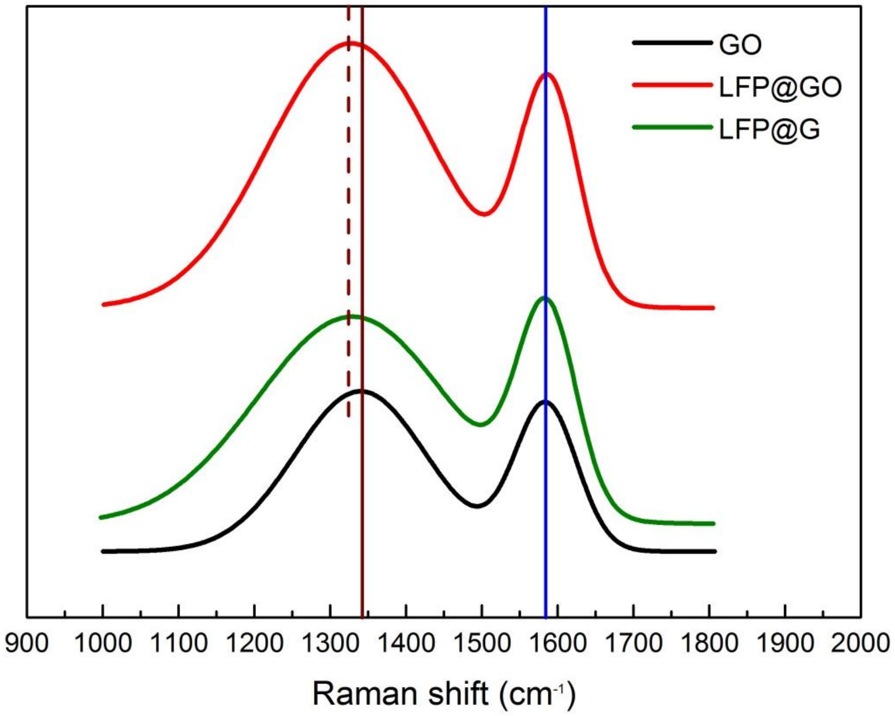

Figure S3.Raman spectra of GO, LFP@GO and LFP@G; the bands in the range of 1200-1460 cm^{-1} and 1470-1730 cm^{-1} are attributed to the *D*-band (K-point phonons of A_{1g} symmetry) and *G*-band (E_{2g} phonons of C_{sp2} atoms)

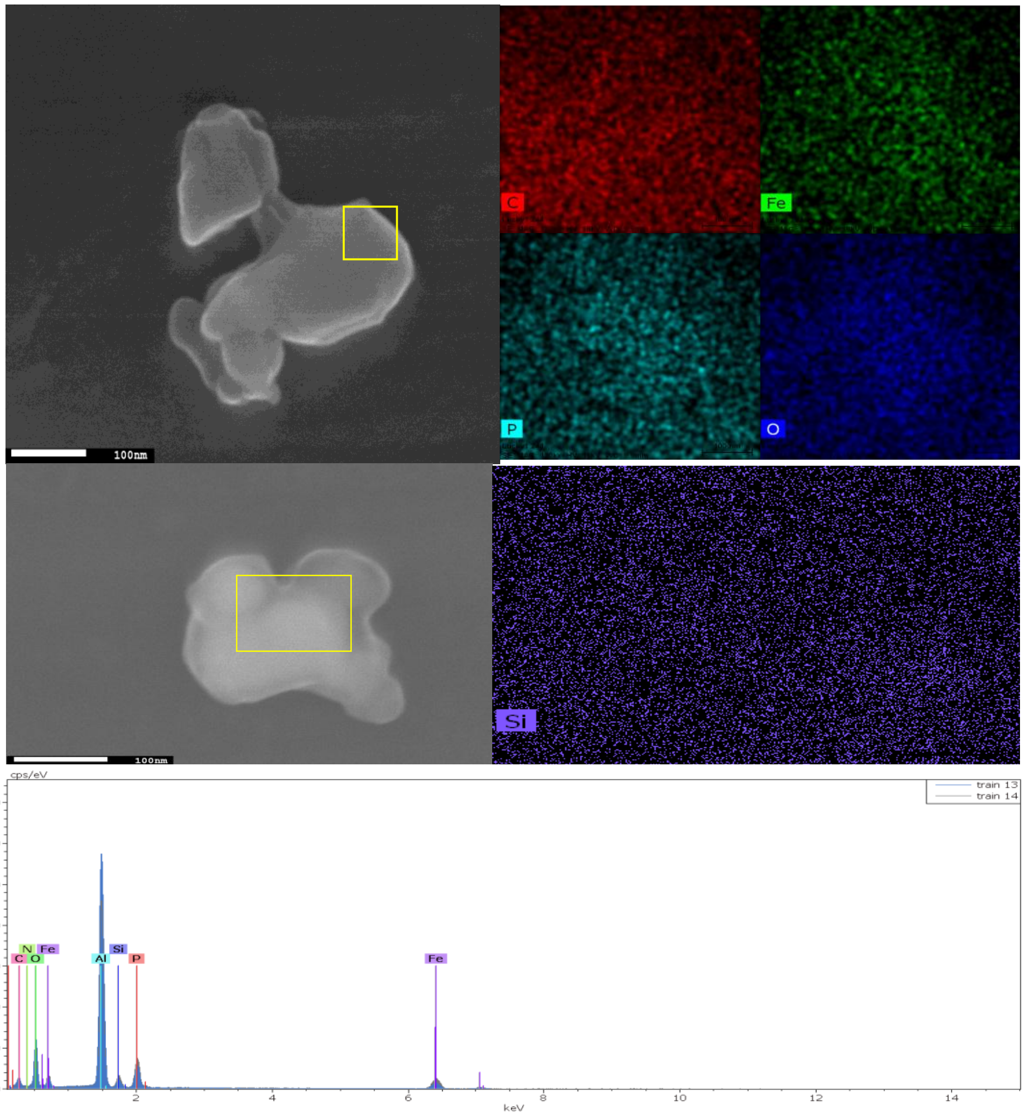

Figure S4. EDS mapping of LFP@G composites.

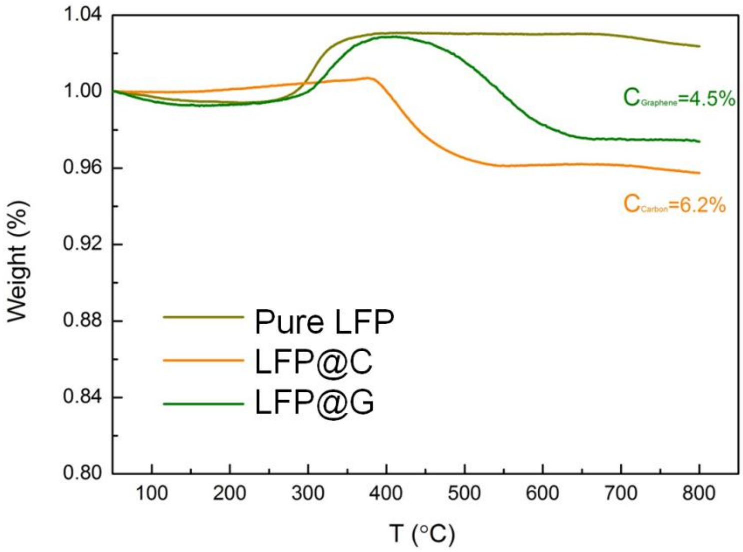

Figure S5. TGA curves of LFP@C and LFP@G composites.

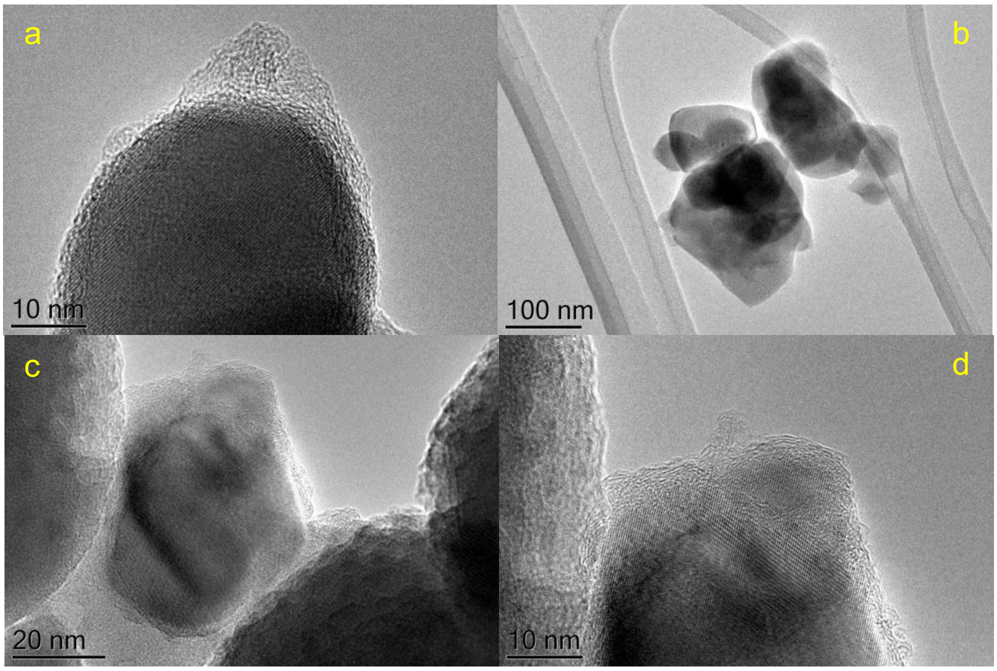

Figure S6. HRTEM images of LFP@G

Electrochemical Characterization

The impedance curves show one condensed semicircle in the medium-frequency region, which could be assigned to the reaction resistance, and an inclined line in the low-frequency range, which could be considered to be Warburg impedance. R_S is the effective resistance due to electrolyte impedance and electrical contacts, and is obtained from the intercept of the semicircle at high frequency with the x-axis. W is the Warburg impedance seen as a sloping line in the low frequency regime, which is associated with Li^+ ion diffusion in the bulk of the electrode. The mid-frequency semicircle is fitted with two depressed semicircles, corresponding to (R_f || CPE1) and (R_{ct} || CPE2), where CPE1 and CPE2 are constant phase elements, which can be attributed to the complex charge transfer processes from the electrolyte to the electrode material. It is suggested that R_{ct} refers to the charge transfer resistance, while R_f is an elevated resistance in the high frequency region associated with the Li^+ ion transfer process at the electrode/electrolyte interface. The exchange current (i_0) and the apparent activation energy (E_a) for the lithium intercalated into the active materials can be calculated from Eq. (1) [2] and the Arrhenius equation, Eq. 2 [2], respectively.

$$i_0 = RT / \mathrm{n}FR_{ct} \qquad (1)$$

$$i_0 = A\exp(-E_a / RT) \qquad (2)$$

where A is a temperature-independent coefficient, R is the gas constant, T (K) is the absolute temperature, n is the number of transferred electrons, and F is the Faraday constant.

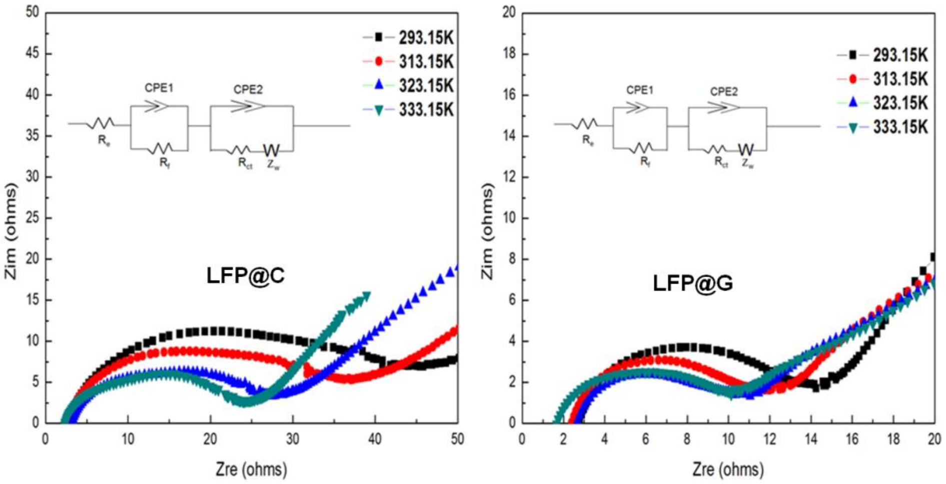

Figure S6. Nyquist plots of LFP@C and LFP@G at a cathodic potential of 4.41 V vs. Li/Li$^+$ at different temperatures. The insets show the equivalent circuit.

The EIS can also be used to calculate the lithium diffusion coefficient using the following Equation (3) ^{2}.

$$D = R^2T^2 / 2A^2\mathrm{n}^4F^4C^2\sigma^2 \quad (3)$$

where R is the gas constant, T is the absolute temperature, A is the surface area of the cathode, n is the number of electrons transferred in the half-reaction for the redox couple, which is equal to 1, F is the Faraday constant, C is the concentration of Li ions in the solid (4.37 × 10^{-3} mol cm^{-3}), D is the diffusion coefficient (cm^2 s^{-1}), and σ is the Warburg factor, which is relative to Z$_{re}$. σ can be obtained from the slope of the lines in Fig. S7.

$$Z_{re} = R_S + R_f + R_{ct} + \sigma\omega^{-1/2} \quad (4)$$

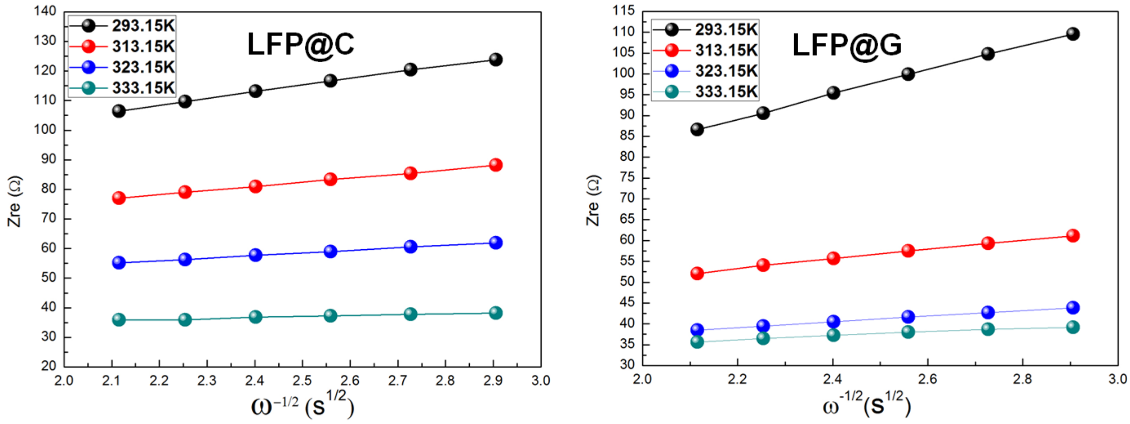

Figure S7. Real parts of the complex impedance versus $\omega^{-1/2}$ at different temperature at a cathodic potential of 4.41 V (vs. Li/Li$^+$)

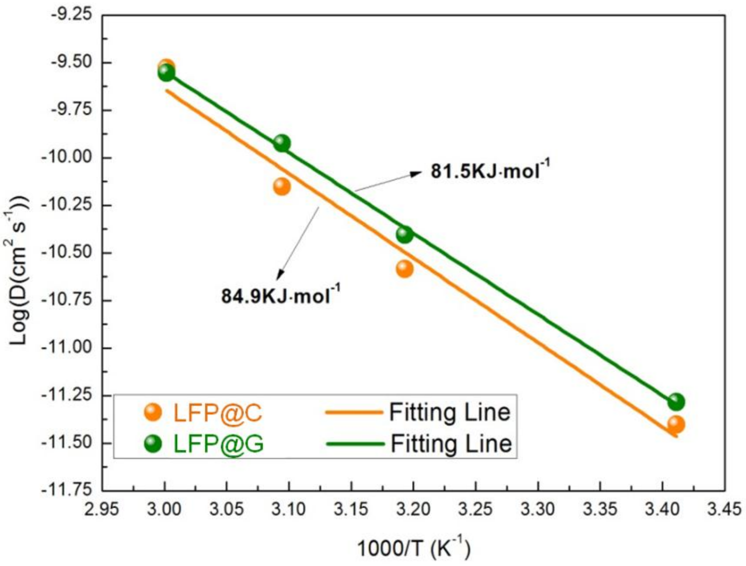

Figure S8. Log *D* versus 1/T plot during lithium insertion at a cathodic potential of 4.41 V (vs. Li/Li$^+$)

1. W. S. Hummers and R. E. Offeman, *J Am Chem Soc*, 1958, **80**, 1339-1339.
2. N. Takami, A. Satoh, M. Hara and I. Ohsaki, *J Electrochem Soc*, 1995, **142**, 371-379.